Journal of Chromatography, 352 (1986) 35–66
Elsevier Science Publishers B.V., Amsterdam — Printed in The Netherlands

CHROMSYMP. 730

HIGH-PERFORMANCE LIQUID CHROMATOGRAPHY OF AMINO ACIDS, PEPTIDES AND PROTEINS

LXVII*. EVALUATION OF BANDWIDTH RELATIONSHIPS OF PEPTIDES RELATED TO HUMAN β-ENDORPHIN, SEPARATED BY GRADIENT-ELUTION REVERSED-PHASE HIGH-PERFORMANCE LIQUID CHROMATOGRAPHY

MILTON T. W. HEARN* and M. I. AGUILAR
St. Vincent's Institute of Medical Research, 41 Victoria Parade, Fitzroy, Melbourne 3065 (Australia)

SUMMARY

The bandwidths of several polypeptides related to human β-endorphin have been investigated with different *n*-alkylsilica stationary phases and different elution gradients of 0.1% trifluoroacetic acid–water–acetonitrile mobile phases. In particular, we have examined the influence of changes in the gradient steepness parameter, *b*, on peakwidth with five different octadecylphases, chemically bonded to porous spherical silica particles of nominally 4 μm and 6 μm average particle diameter, respectively. The effect on the zone dispersion of these polypeptide solutes as the average pore diameter of the silica matrix was increased from 7.3 nm to 30 nm with stationary phases of similar ligand densities packed into columns of identical configuration has been further documented. The experimental data on solute bandwidths and peak capacities are comparable with the corresponding bandwidth and peak capacity values calculated from analytical equations, derived from the general plate height theory and from gradient elution theory. These comparisons clearly demonstrate that anomalous bandbroadening phenomena may occur when polypeptides are eluted with steep gradients, *i.e.* with gradients of large *b* values. Moreover, as the relative chromatographic residence times of β-endorphin peptides capable of forming a C-terminal amphiphilic secondary structures is increased, *i.e.* as the dwell times and median capacity factors, $\bar{k}$, for such peptides are increased, significant divergencies arise between the observed peakwidth behaviour and the behaviour predicted by analytical relationships which describe either the dependency of peak bandwidth (as $4\sigma_v$) on the gradient steepness parameter, *b*, or the dependency of peak capacity on gradient time, t_G, median capacity factor, $\bar{k}$, and the Knox parameter, *C*, respectively. The importance of these divergences from the predicted bandwidth and peak capacity behaviour for polypeptides separated on reversed phases, and for resolution optimisation in particular, is evaluated. These investigations thus enable further assessment of the quantitative relevance of current models that describe polypeptide zone mi-

* For part LXVI see ref. 24.

0021-9673/86/$03.50

gration under gradient elution reversed-phase chromatographic conditions in which solute-dependent slow equilibria, mediated by conformational or solvation effects, may still occur.

INTRODUCTION

The separation of polypeptides and small proteins by gradient-elution reversed-phase high-performance liquid chromatography (RP-HPLC) has gained wide popularity over the past several years. To a very large extent the technique has revolutionised the ultramicro-isolation of many biologically active polypeptides, present in biological extracts in very low natural abundance, such as hormonal polypeptides, growth factors, or lymphokines. In the area of structural elucidation of proteins by peptide mapping and for the analysis of the purity of synthetic peptides, skilful application of different RP-HPLC methods has led to numerous major advances in our knowledge about biological systems (for compendia of recent applications and reviews, see refs. 1–8).

In a typical RP-HPLC separation, a complex mixture of polypeptides will usually be chromatographed on a *n*-alkylsilica stationary phase under gradient elution conditions. This practical requirement arises, in part, from the pronounced dependency of the relative retention and bandwidth of polypeptides and proteins on the volume fraction, φ, of the organic solvent modifier. One manifestation of these dependencies is the very steep slopes (with slope or S values typically greater than 10) found in the linearised plot of the logarithmic capacity factor ($\log k'$) *versus* φ and corresponding large changes in reduced plate heights, h, over relatively small ranges of $\Delta\varphi$. Because of the small diffusion coefficients of polypeptides and proteins in water–organic solvent mobile phases, the observed plate numbers, N, are significantly smaller and, hence, the h values proportionally larger than the N values obtained with low-molecular-weight organic molecules separated under equivalent reversed-phase conditions. However, other effects, mediated by the silanophilic properties of the heterogeneous *n*-alkyl-modified stationary phase surface, by specific solvation or buffer interaction equilibria, and by conformational phenomena, can all contribute to the bandwidth dependencies of these polyionic solutes on experimental conditions. Although it is frequently assumed that all the solute components in a complex mixture can in principle be eluted with well-designed gradient systems from a given column with the same relative bandwidth, careful examination of actual chromatograms for polypeptides, separated on reversed-phase columns under the same gradient conditions of t_G, F and $\Delta\varphi$, usually reveal that this requirement, important though it may be for the optimisation of resolution, is rarely achieved in practice. Similarly, under many isocratic elution conditions, bandwidths are often much larger for polypeptides than would be intuitively anticipated for solutes of similar diffusion coefficients. A change in the mole fraction of the organic modifier by a few percent can result in large increases in peak asymmetry factors, *e.g.* with phenylalanine oligomers a 10% change in organic solvent content results in a *ca.* two-fold change in peak asymmetry[9]. Furthermore, when gradient conditions are changed experimentally, the bandwidths of peptidic components in a mixture may appear from casual inspection not to vary in an equivalent manner as could be an-

ticipated from intuitive considerations of the effect of the gradient parameter on the kinetic behaviour of smaller molecules of similar polarity. Similarly, variations in the bandwidths of polypeptides as the column conditions are changed may not immediately appear to be correlated in a manner expected for the change in a particular feature, such as a column configuration, or change in a bulk property of the stationary phase, such as whether or not extensive end-capping has been employed. For example, some RP-HPLC studies[10–14] have suggested that the chain length of the *n*-alkyl ligand has a major influence on the bandwidth of polypeptides separated under isocratic and gradient elution, whereas other studies[15–21] have concluded that it is the hydrocarbonaceous ligand density rather than the ligand chain length *per se* that influences bandshape. The chemical nature of the hydrocarbonaceous ligand is also well known[5–8,22] to influence resolution, *e.g.* elution profiles of proteins chromatographed on phenyl or diphenyl stationary phases frequently show major differences to those found with *n*-alkylsilica supports. Clearly, it is important to distinguish between superficial differences in the apparent bandwidth behaviour of solutes, which arise as a consequence of the investigations having been carried out in different laboratories with different solutes separated on different stationary phases, derived from silicas of different origin and ligand bonding procedure, and actual solute-dependent differences in bandwidth behaviour, which arise from secondary retention or conformational processes in well-defined chromatographic systems.

The present study is specifically addressed to an analysis of these issues. In particular, the bandwidth behaviour of several polypeptides related to human β-endorphin has been examined as a function of several different column and stationary-phase characteristics, under different conditions of gradient elution. Furthermore, the experimental data for bandwidth, peak capacity and relative retention have been evaluated quantitatively in terms of analytical relationships derived from the general plate height theory and from the theory of gradient elution. Comparisons of the experimental data with the predicted values for the bandwidths and peak capacities of these polypeptides, separated on octadecylsilicas over a wide range of gradient *b* values, reveal solute-dependent divergencies that cannot be readily accommodated by current theoretical treatments based on the assumption that each polypeptide can be represented either by a single, conformationally stable species or by a time-averaged structure of very rapidly interconverting conformers. A conclusion that can be drawn from these findings on the kinetic behaviour of these human β-endorphin-related polypeptides, separated under the chromatographic conditions employed here, is that sequence-dependent re-orientation and conformational transitions of relatively slow relaxation times must be expected to be a common feature of the reversed-phase separations of polypeptides and proteins. Recognition of such "surface shuffling" behaviour, which characterises the propensity of a specific polypeptide to form stabilised α-helical, α-helical–β-sheet, or β-sheet structures at the stationary phase surface, thus introduces a new dimension to the RP-HPLC separation of polypeptides, and biopolymers in general.

EXPERIMENTAL

Chemicals and reagents

Water was quartz-distilled and deionised in a Milli-Q system (Millipore, Bed-

ford, MA, U.S.A.); acetonitrile was HPLC-grade, obtained from Millipore (Lane Cove, Australia); trifluoroacetic acid was obtained from Pierce (Rockford, IL, U.S.A.). The human β-endorphin analogues were generously provided by Dr. Jan van Nispen (Organon, Oss, The Netherlands) and were repurified by semi-preparative reversed-phase chromatography immediately prior to use.

Apparatus

The chromatographic data were collected with a Waters gradient system, consisting of two Model M6000A solvent-delivery pumps, a U6K universal chromatographic injector, a Model M450 variable-wavelength UV monitor, operating at 210 nm, coupled to a Hewlett-Packard 3390A plotter–integrator. Gradients were generated with a precalibrated Waters M660 solvent programmer. Sample injections were made with SGE Model 50A syringes (Melbourne, Australia). The pH measurements were performed with a Radiometer PHM64 meter, equipped with a combination glass electrode.

Chromatographic procedures

Chromatographic measurements were made using 25 cm × 4.6 mm I.D. stainless-steel columns, packed with different developmental dimethyloctadecylsilica with a mean particle diameter of 6 μm and specific surface areas of 380 m^2/g, 177 m^2/g, 143 m^2/g, and 45 m^2/g, with corresponding average pore sizes of 7.3 nm, 10.0 nm, 13.0 nm, and 30.0 nm and alkyl-chain coverages of 2.2, 2.2, 2.0, and 3.1 $\mu mol/m^2$, respectively. The NovaPak C_{18} stationary phase, with a mean particle diameter of 4 μm and a corresponding average pore size of 9.0 nm and alkyl-chain coverage of 3.0 $\mu mol/m^2$, was obtained as prepacked stainless-steel columns (15 cm × 3.9 mm I.D.) or radial compression cartridges (10 cm × 8.0 mm I.D.) from Waters Assoc. (Milford, MA, U.S.A.). Sample sizes for each polypeptide in mixtures varied between 1 and 10 μg, with injection volumes of 10–100 μl. The column dead-time was calibrated with sodium nitrate. All experimental measurements of gradient retention time and peakwidth were repeated at least in triplicate, using scale expansion and cursor techniques that allowed highly reproducible determinations to be made. Experimental bandwidths were corrected for extra-column effects by established procedures. Similarly, gradient retention times were corrected for gradient elapse effects, as described previously[23,24]. Input values of t_o, t_g, t_s, t_G, V_m, x, $\Delta\varphi$, η, MW, T, d_p, F, a', $\sigma_{v,exp}$, d_s, d_q, α, and L, were used in the calculation of the various chromatographic parameters, b, S, k'_o, $\bar{k}$, $\bar{\varphi}$, PC_{exp}, PC_1, PC_2, C, D_m, b', ρ^*, σ_{v1}, σ_{v2}, G, ρ, β, υ, h, and D_s, using composite multivariate linear and non-linear regression best-fit routines with the Chained Pekinese programme, developed in this laboratory and written in BASIC language for a Hewlett-Packard HP86B computer and HP7470A plotter. The standard deviation of fit of the plotted curves and the experimental data was $\leq \pm 10\%$ (1 S.D.). The viscosity values (η) for water–acetonitrile eluents were calculated according to ref. 25. The input value of the column tortuosity factor (γ) was assumed to equal 0.64 for all columns. Similarly, the input dispersion factor (a') was set equal to 1.1, and the restricted diffusion parameter (d_s/d_q) used in eqn. 22 was taken to be smaller than or equal to 0.1. The surface diffusion term (b') and the restricted diffusion term (ρ^*) where derived from linear regression analysis, as were the intercept values of the coefficients (d, e, etc.). Gradient times (t_G) of 20, 30, 40,

60, and 120 min were used at a mobile phase flow-rate of 1.0 ml/min. All chromatographic measurements were carried out at 20°C.

RESULTS AND DISCUSSION

Theoretical considerations

Under chromatographic conditions of gradient elution the resolution between two adjacent peptide zones can be defined as

$$R_{s,i/j} = (\bar{\alpha}_{i/j} - 1)\, N^{1/2}\, [\bar{k}_i/(1 + \bar{k}_i)] \quad (1)$$

where $\bar{\alpha}_{i/j}$ is the gradient separation factor (selectivity) between the two peptides, P_i and P_j, and is equivalent to $\bar{k}_i/\bar{k}_j$; $\bar{k}_i$ and $\bar{k}_j$ are the instantaneous capacity factors for the solutes P_i and P_j as they traverse the midpoint of the column, and N is the theoretical plate number. Furthermore, the peak capacity (PC) for a chromatographic separation of gradient time, t_G, and average resolution, $R_s = 1$, for all adjacent peaks can be expressed by

$$PC = t_G/4\sigma_t \quad (2)$$

where $4\sigma_t$ is the bandwidth in time units for the eluted zone at baseline.

It is now well recognised from experimental and theoretical studies with low-molecular-weight organic solutes that in gradient elution the median capacity factor, $\bar{k}$ (instantaneous capacity factor as the solute traverses the midpoint of the column), and the bandwidth, $4\sigma_t$, of solutes undergoing regular linear elution development on reversed-phase columns are both inversely related to the gradient steepness parameter, b. Although similar inverse proportionalities between $\bar{k}$ and b have recently been verified[23,24,26,27] for polypeptides and proteins separated under reversed-phase and hydrophobic-interaction chromatographic gradient conditions, the question remains whether the bandwidths of polypeptides and proteins follow the same theoretical dependencies on b that are found with low-molecular-weight solutes. By definition, the value of b in linear-solvent-strength gradients[28] is constant for all solutes. However, this requirement is rarely achieved in reversed-phase separations of polypeptides with simple linear-slope time-based gradient conditions. Under regular reversed-phase gradient conditions, *i.e.*, under elution conditions where the average relaxation times[29], τ_i, of specific solvation, conformational, aggregative, or other solute-dependent secondary equilibrium processes are very small compared with the analysis time (t_g), the relationship between the bandwidth and the gradient steepness parameter can be expressed as

$$\sigma_t = (1 + 1/2.3b)\, G t_o N^{-1/2} \quad (3)$$

where t_o is the column dead-time and G is the band compression factor, which arises as a consequence of the increase in solvent strength across the solute zone as the gradient develops along the column. When the initial solvent A condition of the gradient is chosen such that the capacity factor of the solute in solvent A is large, *i.e.* when $k'_0 \gg 1$, the relationship between G and b can be given[28] by

$$G^2 = [1 + 2.3b + 1/3(2.3b)^2]/(1 + 2.3b)^2 \quad (4)$$

Hence, the calculation of σ_t (or alternatively σ_v, since $\sigma_v = \sigma_t F$) for a particular peptide solute separated under a defined gradient condition on a specified column of known t_o requires determination of only the corresponding value of b value and the value of the apparent plate number, N. When the numerical value of σ_t (or σ_v) has been determined, the value of $(PC)_{calc}$ can be found from eqn. 2 for any particular peptide solute separation of defined gradient time, t_G.

For a given column and fixed flow-rate the parameter b is proportional to the change in the volume fraction of the organic solvent modifier per unit time, Θ', and inversely proportional to the gradient time, t_G. The dependence of b on these two experimental variables can be expressed in the form

$$b = St_o\Delta\varphi/t_G = SV_m\Theta'/F \tag{5}$$

where the solute-dependent variable, S, represents the change in the logarithmic capacity factor of the solute over a defined range of the volume fraction of the organic solvent modifier, *i.e.* $S = \Delta\log k'/\Delta\varphi$. The value of S for a particular polypeptide can thus be evaluated from either isocratic or gradient retention data. For convenience these data are usually presented in the form of plots of log k' *versus* φ or log $\bar{k}$ *versus* $\bar{\varphi}$, respectively. Generally, the plots of log k' *versus* φ for polypeptides have been found[5,7,8,16,30] from isocratic experiments to be curvilinear. Although the relationship between log k' and φ thus must involve at least a quadratic-order dependency, over the retention range of interest in resolution optimisation, *i.e.* over the range $1 < k' < 10$, the dependency of log k' on φ can be approximated to the following linearised expression:

$$\log k' = \log k'_0 - S\varphi \tag{6}$$

Thus in circumstances when the S value of a particular polypeptide is known from earlier isocratic or gradient chromatographic studies, the calculation of the b value for different t_G, F or $\Delta\varphi$ values on the same column with the same eluent combinations is straightforward. Empirical relationships[23,24] that link the slope term, S, with molecular weight (MW), such as

$$S = 2.99\,(MW)^{0.21} \approx 3.0\,(MW)^{0.25} \tag{7}$$

or

$$S = 0.48\,(MW)^{0.44} \approx 0.5\,(MW)^{0.5} \tag{8}$$

have recently been derived and can also be used to calculate specific b values. Alternatively, when S and MW are both unknown, the value of b for a particular polypeptide, P_i, chromatographed under a specific gradient condition, can be readily determined from data accumulated from two or more experiments of different gradient times and evaluated[23,24] from the relationship

$$b_i = (t_{o,i}\log\beta)/[t_{g1,i} - (t_{g2,i}/\beta) + t_{o,i}(t_{G1} - t_{G2})/t_{G2}] \tag{9}$$

where $\beta = t_{G2}/t_{G1}$; t_{g1} and t_{g2} are the gradient retention times for the polypeptide P_i, chromatographed with gradient times t_{G1}, and t_{G2}, respectively. Furthermore, the median capacity factor, $\bar{k}$, can be related[28] to b by

$$\bar{k} = \frac{2}{(\ln 10)b} \tag{10}$$

By substituting for b with the other variables in eqn. 5, $\bar{k}$ for an ideal reversed-phase linear-solvent-strength gradient separation can then be expressed in terms of the separation variables t_G, t_o, etc., such that

$$\bar{k} = \frac{2}{(\ln 10)} (Ft_G/SV_m\Delta\varphi) \tag{11}$$

Hence, the value of $\bar{k}$ for any peptidic solute, chromatographed under the criteria of regular reversed-phase elution on a given column under defined gradient conditions, can be calculated from experimentally derived input values of F, t_G, S, $\Delta\varphi$, and V_m. By combining eqns. 3 and 10 and by substituting $\sigma_v = F\sigma_t$, the following relationships between σ_v and $\bar{k}$ are derived, namely:

$$\sigma_v = (\bar{k}/2 + 1)Gt_oN^{-1/2}F \tag{12}$$

and, since $t_oF = V_m$, then

$$\sigma_v = (\bar{k}/2 + 1)GV_mN^{-1/2} \tag{13}$$

When such ideal separations occur with each zone being eluted with regular reversed-phase selectivity as a gaussian peak, the bandwidth σ_v can alternatively be defined as

$$\sigma_v = t_GF(1 + 1/\bar{k})/(\ln 10)N^{1/2}S\Delta\varphi \tag{14}$$

Retention data from several gradient runs allow $\bar{k}$ and S for a specific t_G to be derived and their values to be inserted into eqn. 14. Furthermore, for a given column and a fixed flow-rate, the remaining term in eqns. 12–14, the apparent plate number N, can be evaluated from the general plate-height theory. Thus under conditions of linear-elution chromatography and in the absence of slow secondary equilibria, the rate of dispersion of the solute zone as a function of the mobile phase flow-rate can be represented by the Knox equation, namely

$$h = Av^{1/3} + B/v + Cv \tag{15}$$

where h is the reduced plate height (equal to L/Nd_p) and v is the reduced velocity, as defined by

$$v = LFd_p/V_mD_m \tag{16}$$

where L is the column length, d_p is the mean particle diameter, and D_m is the diffusion coefficient of the solute in the mobile phase. Since the peak variance, σ_t^2, due to chromatographic effects is given by

$$\sigma_t^2 = \frac{hd_p}{L} t_g^2 \tag{17}$$

then the change in bandwidth (*i.e.* change in $4\sigma_t$ or $4\sigma_v$) of an eluted solute zone of retention time t_g will be dependent on the average diffusion coefficient of the solute in the mobile phase, the average size of the particles, the quality of the column packing, and indirectly, the pore size, the ligand density, and the uniformity of the stationary-phase surface. In fact, the A term of the Knox equation accommodates effects due to eddy diffusion and non-uniform linear velocities of the solute zone and the mobile phase as a consequence of packing irregularities. For well-packed columns containing particles of narrow size distribution and small average particle diameters, typical values of A range between 0.5 and 1.0. Clearly, the smallest possible value of A is desirable, since this permits the use of higher flow velocities and shorter columns. The B coefficient of the Knox equation arises from dispersion contributions of the solute zone in both the mobile phase and the stationary phase and accounts for the rate at which the solute diffuses in the column. The B coefficient is proportional to the diffusion coefficient and can be represented by

$$B = 2\gamma D_m \tag{18}$$

or

$$B = a' + b'k \tag{19}$$

where the obstruction factor, γ, is typically between 0.6 and 1.0 and arises from the complexity of the packing structure, the dispersion term a' is typically 1.1, the surface diffusion parameter, b', is related to D_s/D_m and varies between 0 and 0.5, and D_s is the diffusion coefficient in the stationary phase. Empirically, the surface diffusion parameter, b', is dependent on molecular weight, and this relationship can be expressed in the form $b' = d - e \log(\mathrm{MW})$. As the flow-rate increases, or as the residence time in the column decreases, *i.e.* as $\bar{k}$ becomes smaller, band-broadening of the migrating solute zone due to contributions from the B coefficient will decrease. As can be seen from eqn. 19, the B coefficient is effectively a function of the molecular properties of the solute, its value being largely determined by the diffusion coefficients, D_s and D_m. Stationary-phase-surface or pore-chamber effects, which dramatically change the apparent value of D_s of a peptide solute or which lead to multizoning phenomena, will thus be reflected in variations in the B coefficient.

The B coefficient will thus respond to solute changes in conformation, if random-coil, β-barrel or α-helical secondary structural changes occur, *i.e.* in situations where solute structures alternate with relatively slow relaxation times between, *e.g.*, pseudo-spherical and pseudo-cylindrical forms in the intraparticulate regions or at the stationary-phase surface.

Since the values of υ in a typical gradient experiment are usually large for

peptide and protein separations on reversed-phase columns, h is frequently not very sensitive to changes in the values of either the A or the B term. As a consequence, with well-packed columns, operated at relatively high linear flow velocities, the $Av^{1/3}$ and the B/v terms of the Knox equation can largely be ignored for polypeptides separated on reversed-phase columns by isocratic or gradient elution. In contrast, the C term, which accounts for the resistance to mass transfer at the stationary phase surface inside the pores of the column packing, varies significantly with separation conditions. Thus, any change in the value of C will have a significant effect on h. In gradient elution, the dependence of C on separation conditions can be represented by

$$C = [(1 - x + \bar{k})/(1 + \bar{k})]^2/15\rho^* (B - 1.28x) \tag{20}$$

where

$$B = 1.28x + \frac{D_p}{D_m}(1 - x) \tag{21}$$

and x is the fraction of the mobile phase outside the pores of the particle; the obstruction factor, γ, here has been set equal to 0.64, and ρ^* is the restricted diffusion parameter, as defined by the Renkin relationship[31]

$$\rho^* = 1 - 2.104\rho + 2.09\rho^3 - 0.95\rho^5 \tag{22}$$

where ρ is the ratio of the Stokes diameter of the solute (d_s) to the pore diameter of the particle (d_q), and D_p is the effective intraparticle diffusion coefficient. The parameter ρ^* thus depends on the molecular weight and the Stokes diameter of the solute and the average diameter, d_q, of the stationary phase pores. When the Stokes diameter of the solute is similar to the pore diameter, diffusion is restricted, and D_p is decreased. The change in D_p as a function of ρ^* can be expressed as

$$D_p = D_m\rho^*/2.1 \tag{23}$$

In order to prevent exclusion from interstitial channels, it has been concluded by Giddings[32,33] that for SEC packings the ratio of the diameter of the largest internal pores to the diameter of the narrowest channels should be significantly less than 0.25. Similar criteria appear relevant also to reversed-phase packings. Furthermore, based on theoretical considerations and experimental findings[16], the particle diameter and the pore diameter should be larger than the Stokes diameter of the solutes by factors of at least 50–100 and 10–15, respectively. Various preparations of porous spherical or irregular silicas with such physical characteristics have been available in the particle diameter range 5–10 μm for several years. For small polypeptides up to *ca.* 5 Kdaltons, where the d_s for the polypeptide in monomeric form will usually be less than 2 nm, the ρ term ($= d_s/d_q$) of eqn. 22 will be typically less than 0.02 for silica particles with average pore diameters greater than 10 nm. With polypeptides separated on porous *n*-alkylsilicas where the ρ values are 0.1, 0.2, 0.5, and 1, the corresponding values of ρ^* are *ca.* 0.8, 0.6, 0.35 and 0.04, respectively. Thus, porous

particles with mean diameters in the range 4–10 μm and with pore diameters greater than 15 nm appear from geometrical arguments to be much more suitable for separations involving mixtures of small and large polypeptides. Although particles of smaller diameter (*i.e.* less than 3 μm) can also be used, besides the inherent increase in the pressure drop across the column with these smaller particles, decreased resolution of higher-molecular-weight components may arise from exclusion and restricted diffusion effects.

The diffusion coefficients of polypeptides and proteins are typically at least one order of magnitude smaller than those of low-molecular-weight compounds, with D_m for polypeptides and small globular proteins usually less than 10^{-6} cm^2/s. In most cases, the diffusion coefficient of a specific polypeptide solute in a particular mobile phase composition or at the stationary phase surface is not available from the literature. However, a number of empirical expressions that interrelate the diffusion coefficient of a solute (D_m) in solution with its molecular weight and eluent viscosity (η), can be employed to determine D_m, including the Wilke–Chang equation[34], in which D_m is given by

$$D_m = \frac{7.4 \cdot 10^{-10} (\Phi' \mathrm{MW})^{0.5} T}{\eta V_{mv}^{0.6}} \tag{24}$$

or the Stokes–Einstein equation[33] where

$$D_m = \frac{k_c T}{3(\mathrm{MW}) n d_s} \tag{25}$$

or other empirical relationships of the form such as

$$D_m = 8.34 \cdot 10^{-10} \frac{T}{\eta(\mathrm{MW})^{0.33}} \tag{26}$$

and

$$D_m = \frac{9 \cdot 10^{-6}}{\eta} [2.2(\mathrm{MW})^{-0.33} + 62(\mathrm{MW})^{-1}](T/298) \tag{27}$$

where Φ' is an association constant and is near unity for solvents with no hydrogen-bonding capability and has the value 2.7 for water; T is the absolute temperature (in K), η is the viscosity of the eluent; V_{mv} is the molecular volume of the solute; k_c is the Boltzmann constant, and d_s is the Stokes radius of the solute, which is typically *ca.* 108–110% of the molecular radius for globular solutes.

For the polypeptides studied in the present investigations, D_m was computed from eqn. 26, with appropriate values of MW, η, and T. The choice of this equation to calculate D_m was based on our investigations with other polypeptides and small globular proteins as well as the recent study by Young *et al.*[35] on the correlation between diffusion coefficients and molecular weights of different proteins, where collectively the experimental diffusion coefficients were found to be within 20% of the predicted value. Because precise values of V_{mv}, Φ', or d_s are generally not available

for a given peptide solute in a particular mobile phase, in order to utilise eqns. 24 and 25, either values for d_s/d_q, V_{mv}, or Φ' must be initially chosen arbitrarily and subsequently refined by iterative methods, or they must be determined by modifications of the Furth and Zuber method and evaluated according to Fick's method for each polypeptide at each eluent composition in unpacked columns so that the values of υ, B, C, and ρ^* can be determined from eqns. 16–22. It is evident from eqns. 20–23 that for a given column and with a polypeptide of specified relative retention, *i.e.* for defined values of x and $\bar{k}$, the surface diffusion and restricted diffusion terms can have significant effects on the magnitude of the Knox C term. These effects become very important in terms of their contribution to bandwidth phenomena with polypeptides, irrespective of whether these polyionic solutes are eluted isocratically or under gradient conditions from microparticulate reversed-phase columns, since high reduced velocities, such as $\upsilon > 100$, are commonly employed. Under these typical flow-rate conditions, *i.e.* when $F \geqslant 1$ ml/min, the dependency of the reduced plate height on the reduced velocity can thus be approximated to

$$h = C\upsilon \tag{28}$$

When these conditions apply, the plate number, N, is given by

$$N = \frac{D_m t_o}{C\, d_p^2} \tag{29}$$

Hence, substitution of this simplified relationship for N into eqns. 13 and 14 yields the following alternative expressions for the bandwidth in volume units, σ_v, for a polypeptide, chromatographed under regular reversed-phase gradient conditions on a porous *n*-alkylsilica support:

$$\sigma_v = (\bar{k}/2 + 1)\, G\, V_m d_p \left(\frac{C}{D_m t_o}\right)^{0.5} \tag{30}$$

or

$$\sigma_v = t_G F\, d_p \left(1 + \frac{1}{\bar{k}}\right) C^{0.5}/(\ln 10)\, S\Delta\varphi (D_m t_o)^{0.5} \tag{31}$$

If the relationship between peak capacity (PC) and σ_v is recalled (eqn. 2), PC can be expressed in terms of the chromatographic variables S, $\Delta\varphi$, N, and $\bar{k}$ such that

$$\mathrm{PC} = \frac{(\ln 10)}{4} (S\Delta\varphi)\, N^{0.5}[\bar{k}/(1 + \bar{k})] \tag{32}$$

Hence, by appropriate substitution for N or σ_v, the following expressions for PC are obtained

$$\mathrm{PC} = \frac{t_G\, D_m^{0.5}\, t_o^{0.5}}{4(\bar{k}/2 + 1)\, G\, V_m d_p C^{0.5}} \tag{33}$$

TABLE I

CHARACTERISTICS OF THE POLYPEPTIDES RELATED TO HUMAN β-ENDORPHIN USED IN THE PRESENT STUDY

No.	*Solute**	*MW*	*Number of residues*	$D_m \cdot 10^7$ (cm^2/s)**	*S value****					
					1	*2*	*3*	*4*	*5*	*6*
1	YGGFM	573	5	3.40	7.7	8.6	10.0	10.8	13.7	12.4
2	YGGFMTS	761	7	3.10	9.4	10.5	11.2	12.9	17.8	14.8
3	YGGFMTSEKSQTPLVT	1744	16	2.35	11.6	13.0	14.2	16.7	27.0	23.4
4	YGGFMTSEKSQTPLVTL	1859	17	2.30	11.3	12.6	13.1	14.8	25.2	21.1
5	YGGFMTSEKSQTPLVTLFK	2134	19	2.20	11.5	11.5	13.1	14.3	28.4	25.8
6	YGGFMTSEKSQTPLVTLFKNAIIKNAYKKGE	3263	31	1.92	15.2	15.3	15.1	15.2	45.9	56.6

* The one-letter code for the amino acids is used as suggested by M. O. Dayhoff in *Atlas of Protein Sequence and Structure*, National Biomedical Research Foundation, Silver Spring, MD, 1968.

** The diffusion coefficient, D_m, for the various peptides was calculated from eqn. 26 with the eluent viscosity, η, adjusted for the acetonitrile content, as described in ref. 25.

*** The S values were determined by linear regression analysis according to eqns. 5 and 9. Columns: 6 μm dimethyloctadecyl silicas of 7.3 nm (1), 10 nm (2), 15 nm (3), and 30 nm (4) average pore diameter, packed into 25 cm × 4.6 mm I.D. stainless-steel columns; 4-μm Novapak dimethyloctadecylsilicas, packed into stainless-steel columns (5) (15 cm × 3.9 mm I.D.); radial-compression cartridges (10 cm × 8 mm I.D.) (6).

and

$$PC = \frac{(\ln 10)}{4} \frac{S\Delta\varphi\, D_m^{0.5}\, t_o^{0.5}}{(1 + 1/\bar{k})\, F\, d_p\, C^{0.5}} \tag{34}$$

Since $(1 + 1/\bar{k})$ can be approximated by $1/\bar{k}^{0.25}$, eqn. 34 may be simplified to

$$PC = \frac{(\ln 10)}{4} \frac{S\Delta\varphi\, D_m^{0.5}\, t_o^{0.5}\, \bar{k}^{0.25}}{F\, d_p\, C^{0.5}} \tag{35}$$

Hence, for specific polypeptides, eluted under defined gradient conditions from a given column, linear dependencies between peak capacity and $\bar{k}^{0.25}/C^{0.5}$ are to be expected, provided the elution is characterised by regular reversed-phase retention behaviour with no conformational or other solute-specific secondary solution equilibria participating, *i.e.* that their relaxation time requirements[29] are well outside the limits $1 < \tau_i/t_{g,i} < 10$. Eqn. 35 also predicts that, as the S parameter of the solute increases, PC will proportionally increase. Larger $\Delta\varphi$ values will also favour higher PC values, in accord with experimental observation. Because the B and C terms depend on the magnitude of the pore diameter, it also follows that, as the pore diameter, d_q, increases, PC should increase for specified solutes when all other parameters are held constant. Similarly, as the particle diameter, d_p, decreases, proportional increases in PC are predicted by eqn. 35 without change in analysis time, *i.e.*, at constant values of $\bar{k}$ and t_G, linear inverse relationships of PC on d_p are predicted, provided no change in the D_m/C term occurs.

In order to verify the above relationships with polypeptides, and to provide further insight into the dynamics of polypeptide interactions with hydrocarbonaceous surfaces in general, the bandwidth data for a series of six polypeptides related to human β-endorphin (Table I) have been determined. Firstly, the experimental values of the bandwidth ($4\sigma_{v,exp}$) were compared with the predicted values of the zone bandwidth ($4\sigma_{v,calc1}$ and $4\sigma_{v,calc2}$, calculated according to eqns. 30 and 31, respectively) as a function of the gradient steepness parameter, b. Secondly, peak capacity (PC_{exp}), as calculated from the experimental values of t_G and $4\sigma_{v,exp}$ according to eqn. 2, and peak capacity (PC_{calc}) as calculated according to eqn. 35, were compared as functions of $\bar{k}^{0.25}/C^{0.5}$, D_m being computed from the empirical eqn. 26. With the availability of columns of the same configuration and packed with particles of the same mean diameter and bonded to stationary phases with similar ligand densities, the effects of the pore diameter on PC for these polypeptides, separated under identical gradient conditions, were compared. Collectively, these results were then evaluated in terms of current models for polypeptide and protein retention on microparticulate, chemically bonded, *n*-alkylsilica stationary phases with elution by water–organic solvent gradients at low pH.

Comparison of observed and predicted bandwidths for the human β-endorphin-related polypeptides 1–6

Adsorption of polypeptides on reversed-phase chromatographic packing materials is now believed to be due to the solvophobic expulsion of the solute from the polar mobile phase onto the non-polar stationary phase surface. As a consequence,

the hydrophobic area, occupied by the macromolecule at the stationary phase/mobile phase interface, will predominantly determine the extent of interaction under regular reversed-phase conditions with mono-layer *n*-alkylsilica stationary phases. For convenience of interpretation and prediction of retention data, it has frequently been assumed in reversed-phase chromatography of peptides that the amino acid composition rather than the amino acid sequence of small peptides determines this relative retention. One corollary, which rigorously arises from this assumption, is that each peptide must be represented by an average structure, essentially one in which no unique solute-dependent geometric factors are present and in which the hydrophobic functional group contributions of individual amino acids are independent of the position of the amino acid residue in the molecule.

For small organic molecules, the basis for such first-order approximations have been widely discussed in the literature and have found extensive experimental support in the functional group–relative retention relationships, as described by the Martin equation and related equations based on retention indices. Similar approaches with polypeptides clearly require that the solutes in water–organic solvent combinations in reversed-phase systems are all in the same equivalent average conformational and solvation states. The underlying kinetic processes that lead to the bandbroadening of the solute zones will under these circumstances, be predominantly governed by conventional zone dispersion effects with little or no participation of secondary structural effects and related topographic changes, which arise from conformational reorientation of the solute in the mobile phase or at the stationary phase surface.

Whether or not these ideal conditions apply, the solute zone, as it migrates down the chromatographic column will always be subjected to physical processes of bandbroadening, owing to (1) axial dispersion in the bulk mobile phase, (2) dispersion due to slow mass transfer across the boundary interface and in intraparticulate spaces of the porous particles of the stationary phase, and (3) dispersion due to slow mass transfer of the solute zone from a quantitatively heterogeneous stationary phase surface. Each of these dispersion effects can now be adequately described in terms of the established theory of bandbroadening in the case of rigid conformational species. Thus, if the retention process for polypeptide and protein adsorption in RP-HPLC simply involves the reversible binding of conformationally invariant but sequentially different hydrophobic regions at the surface of these polar solute molecules (P_i) to accessible non-polar ligands (L_o) at the stationary phase surface without subsequent molecular re-orientation, *i.e.*, if the retention process can be described by

$$P_{i,f} + nL_{o,f} \rightleftharpoons P_{i,b} + mL_{o,b} \tag{36}$$

where the subscripts f and b refer to free and bound solvated forms of P_i and L_o, respectively, and the conditions of linear-elution chromatography apply, *i.e.* for gradient elution, $\bar{k}$ is independent of sample size, $h \approx Cv$ for large v values and small D_m values, and the selectivity is controlled solely through solvophobic phenomena, then good correlation between experimental bandwidths and bandwidths predicted by eqns. 30 and 31 would be expected for different gradient conditions, irrespective of the particle diameter or the pore diameter of the stationary phase.

As the dynamic behaviour of a polypeptide approaches that predicted by the simple model represented by eqn. 36, the value of $\sigma_{v,exp}/\sigma_{v,calc}$ is expected to approach

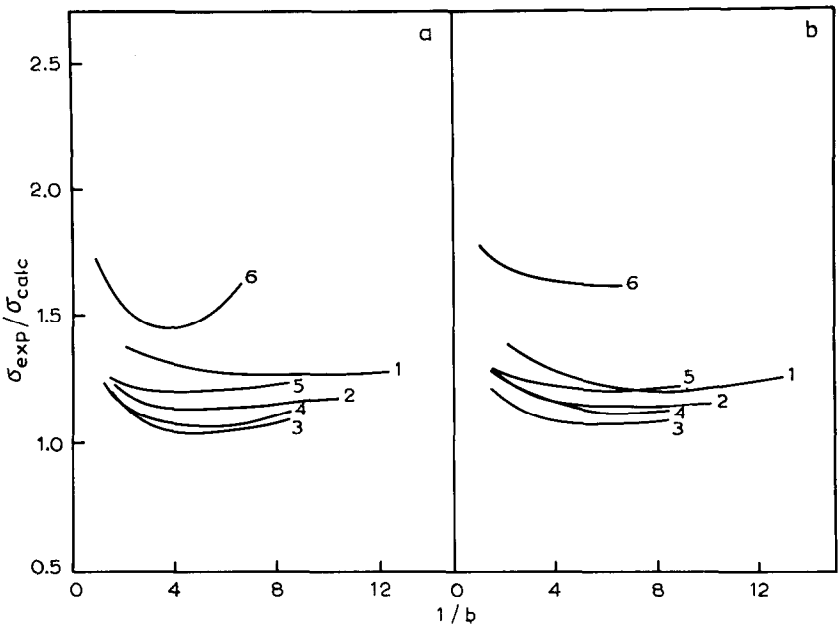

Fig. 1. Plot of $\sigma_{v,exp}/\sigma_{v,calc}$ *versus* $1/b$ for the human β-endorphin-related polypeptides 1–6 (Table I). Data acquired under conditions of different gradient time (t_G = 20, 30, 40, 60 and 120 min), but with the same mobile phase composition limits [water containing 0.1% trifluoroacetic acid to acetonitrile–water (50:50) containing 0.1% trifluoroacetic acid] at a constant flow-rate of 1 ml/min. Experiments carried out with 6-μm octadecylsilica with an average pore diameter of 7.3 nm, packed into a 25 cm × 4.6 mm I.D. stainless-steel column. The value of $\sigma_{v,calc}$ is calculated from eqn. 13 (panel a) and eqn. 14 (panel b) and $\sigma_{v,exp}$ was determined for each polypeptide by direct measurement.

unity. When the ratio is less than unity, it follows that the actual D_s or D_m value of the polypeptide in the chromatographic system is much larger (and, hence, the value of the C term is smaller) than predicted by empirical equations which link σ_v, h, D_m and MW. Such a situation could arise when the mobile phase composition induces a solute-specific stabilisation of structure, leading to a decrease in the molecular volume (V_{mv}) of the polypeptide in that particular environment. The effect of glycerol and other polyhydroxylic additives[36] on polypeptide bandshape in high-performance size exclusion chromatography may operate through this mechanism. The decrease in V_{mv} for β-endorphin in the presence of anionic lipids presumably involves a similar phenomenon[37]. More commonly, it could be anticipated that the ratio $\sigma_{v,exp}/\sigma_{v,calc}$ will be greater than unity due to the participation of secondary dynamic effects —of magnitude if not in complexity unique to the solute— which are not recognised by the simple retention and kinetic models discussed above. Figs. 1–6 show the plots of $\sigma_{v,exp}/\sigma_{v,calc}$ for the series of human β-endorphin peptides, separated on octadecylsilicas as a function of the inverse of the gradient steepness parameter, b. It is clearly evident from these figures that, as the magnitude of $1/b$ increases from 1 to 6, the value of $\sigma_{v,exp}/\sigma_{v,calc}$ approaches a minimum. Also noteworthy from these plots is the observation that for small values of $1/b$, *i.e.* for those experiments with steep gradients, the ratio of the experimental bandwidths of all polypeptides examined to the

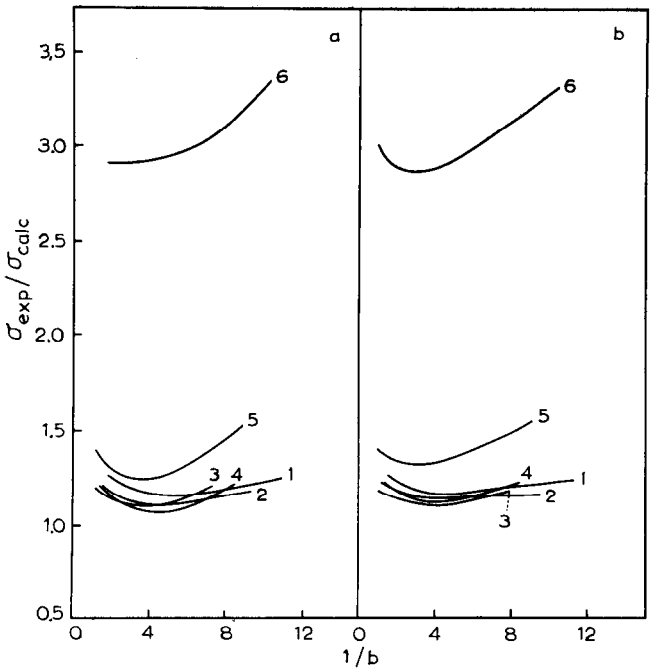

Fig. 2. Plot as in Fig. 1. Details and conditions equal to Fig. 1, except octadecylsilica with an average pore diameter of 10.0 nm.

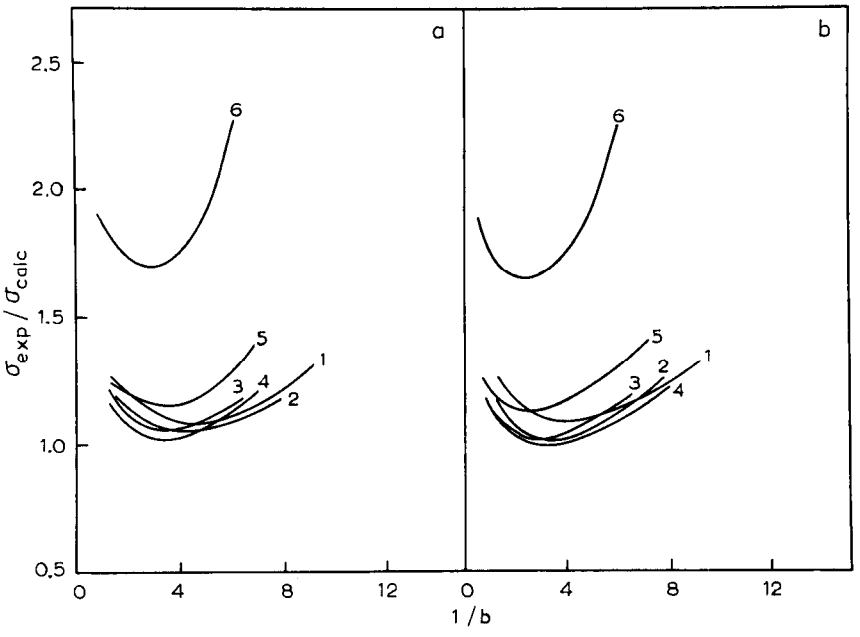

Fig. 3. Plot as in Fig. 1. Details and conditions equal to Fig. 1, except octadecylsilica with an average pore diameter of 13.0 nm.

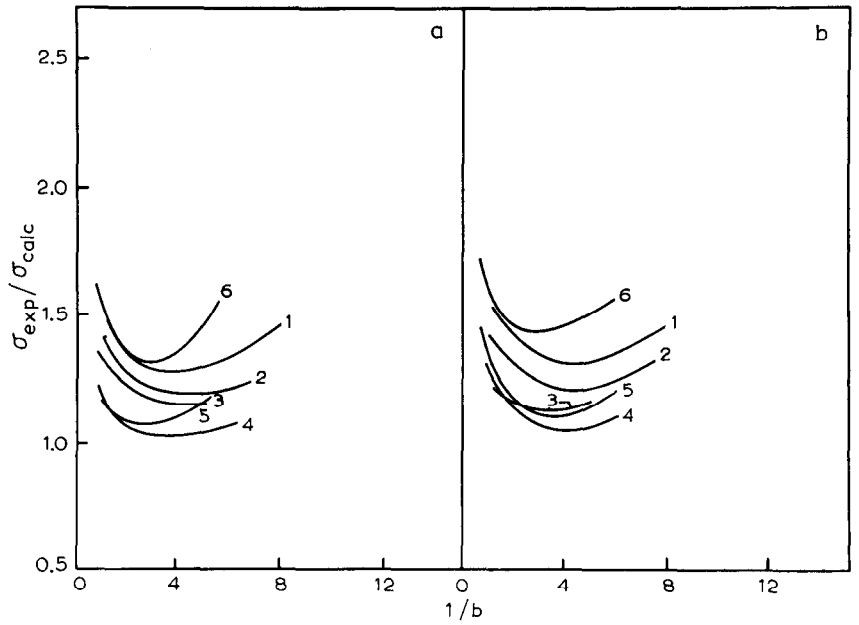

Fig. 4. Plot as in Fig. 1. Details and conditions equal to Fig. 1, except octadecylsilica with an average pore diameter of 30.0 nm.

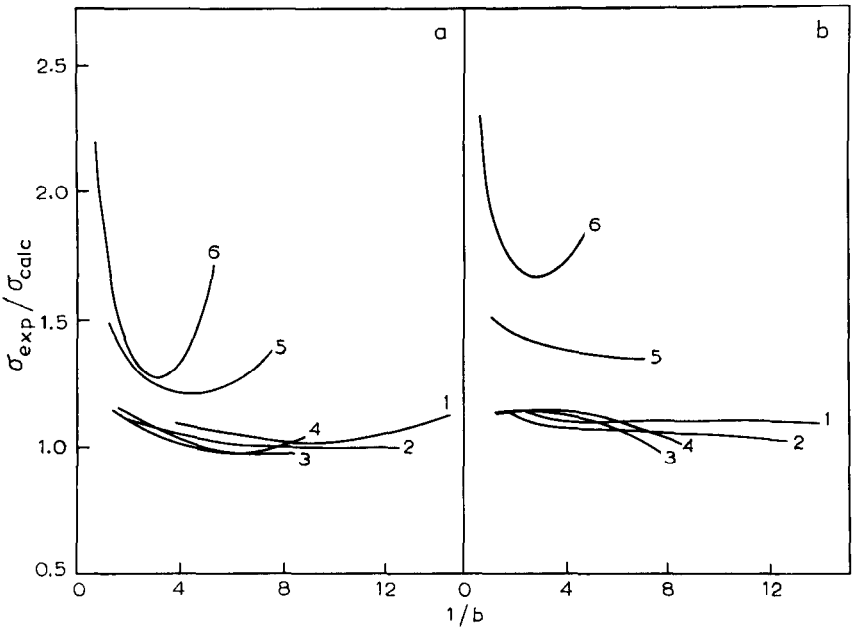

Fig. 5. Plot as in Fig. 1. Details and conditions equal to Fig. 1, except experiment carried out with a 4-μm Novapak C_{18} stationary phase, packed into a 15 cm $\times$ 3.9 mm I.D. stainless-steel column.

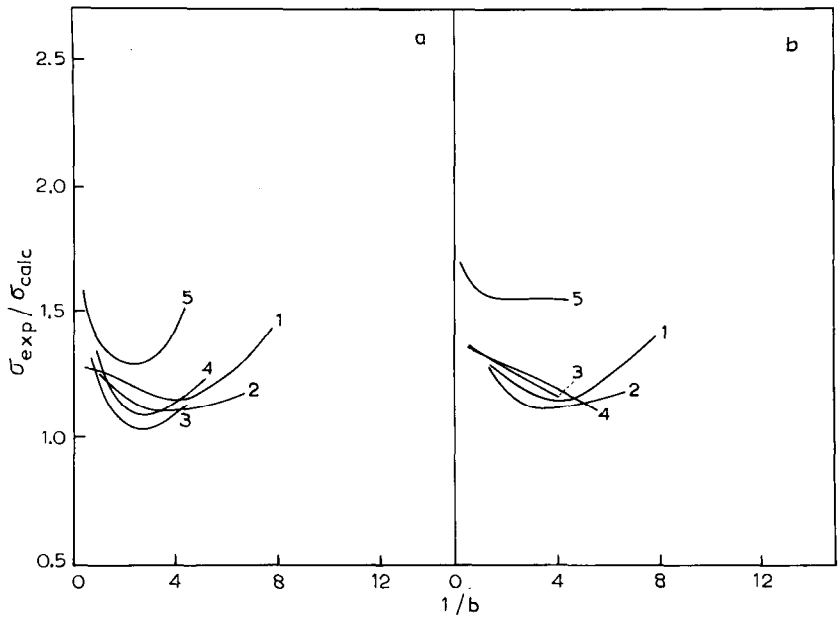

Fig. 6. Plot as in Fig. 1. Details and conditions equal to Fig. 1, except experiment carried out with a 4-μm Novapak C_{18} stationary phase, packed into a 10 cm × 8.0 mm I.D. radial-compression cartridge.

predicted bandwidths is in all cases larger than predicted by either eqn. 30 or 31 and increases as the value of b increases. These results are in accord with our other findings[38] on the influence of separation time and gradient slope on the resolution of polypeptides and proteins, separated by reversed-phase and ion-exchange HPLC. Similar bandwidth behaviour has also been noted by other workers for desamidoinsulin[39], viral proteins[40], peptide hormones[41], and small proteins, such as lysozyme and ribonuclease A[14].

This bandwidth behaviour at large values of b would thus appear to be a general phenomenon, common to both reversed-phase and ion-exchange separations of biopolymers. At very small values of $1/b$ the condition of linear-solvent-strength gradients will no longer be fulfilled, leading to band compression effects which are not adequately predicted by eqn. 4. This affect, coupled with the increasing important effect of the gradient elapse time may provide the explanation for the divergence of $\sigma_{v,exp}$ from $\sigma_{v,calc}$ at small $1/b$ values where essentially step gradients approximating displacement phenomena may occur. Although the origin of this effect remains to be fully elucidated, its recognition is highly relevant to preparative separations[42], where gradients of very steep slope or, alternatively, step-elution programmes are commonly employed.

Further examination of the data in Figs. 1–6 shows that comparable plots of $\sigma_{v,exp}/\sigma_{v,calc}$ *versus* $1/b$ are obtained irrespective of whether eqn. 30 or 31 is used to calculate $\sigma_{v,calc}$. However, the differences in the actual magnitude of $\sigma_{v,exp}/\sigma_{v,calc}$ for the various polypeptides are much more noteworthy. It can be seen that the value of $\sigma_{v,exp}/\sigma_{v,calc}$ is smallest for the small peptides 1 and 2 (YGGFM and YGGFMTS). When allowance for the likely errors inherent in the assumptions made in the deri-

vation of eqns. 30 and 31 are taken into account, the value of $\sigma_{v,exp}/\sigma_{v,calc}$ for the small peptides approaches unity, as anticipated for regular behaviour at larger values of $1/b$, *i.e.* shallower gradients with larger t_G at fixed F. Much more surprising is the bandwidth behaviour of the larger peptides, such as human β-endorphin, where the observed bandwidth is significantly greater than predicted from eqns. 26, 30, and 31 for a globular solute of MW 3263. Clearly, the bandwidth behaviour of this polypeptide on the different stationary phases used in the present study is not consistent with the simple retention model, expressed as eqn. 36.

Furthermore, when an arbitrary value of $N \approx 10\,000$ theoretical plates/m is used rather than the value of N calculated according to eqn. 29 for all the polypeptides (the value of N was found to be $> 20\,000$ theoretical plates for these same columns with low-molecular-weight solutes, such as dansyl or phenylthiohydantoin derivatives of the amino acids) in calculations of $\sigma_{v,calc}$ according to eqns. 12 and 14, the divergencies from unity for $\sigma_{v,exp}/\sigma_{v,calc}$ were even more pronounced. For example, Figs. 7–12 show the plots of $\sigma_{v,exp}/\sigma_{v,calc}$ *versus* $1/b$ for these same polypeptides when this arbitrary value of $N \approx 10\,000$ theoretical plates/m is used, which could be considered indicative of a high-efficiency polypeptide separation. It was obvious from the experimental results that the actual value of N was much smaller than 10 000 theoretical plates. Furthermore, Figs. 1–12 and associated data clearly indicate that it cannot be assumed that the value of N will be constant for different polypeptides, even of similar molecular weight and sequence, when chromatographed under the same conventional gradient elution conditions on *n*-alkylsilicas. As a codicil, the use of a common N value for different peptide solutes, separated under gradient conditions, clearly will lead to erroneous interpretation of bandwidth dependencies on

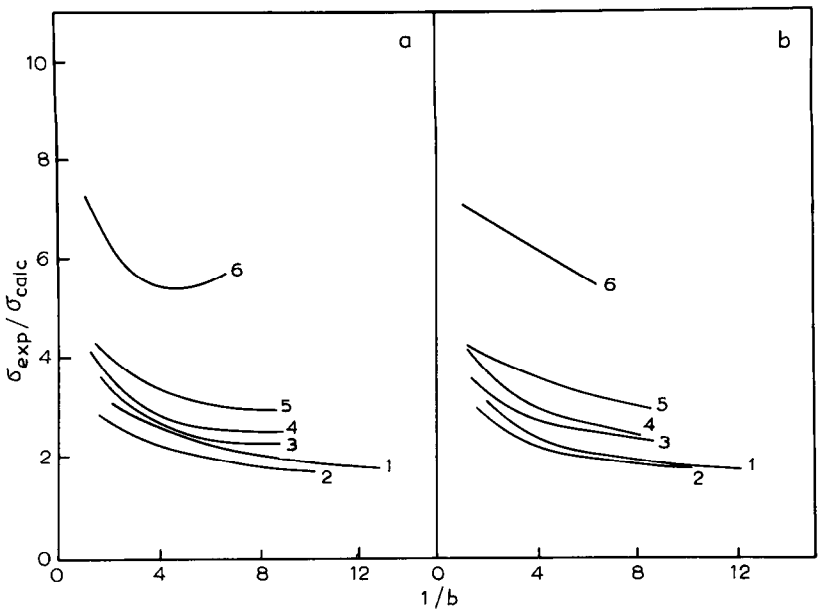

Fig. 7. Plot as in Fig. 1. Details and conditions equal to Fig. 1, except that $\sigma_{v,calc}$ is calculated on the assumption that a constant value of N (= 10 000 theoretical plates) occurred for all polypeptides eluted under conditions of different t_G.

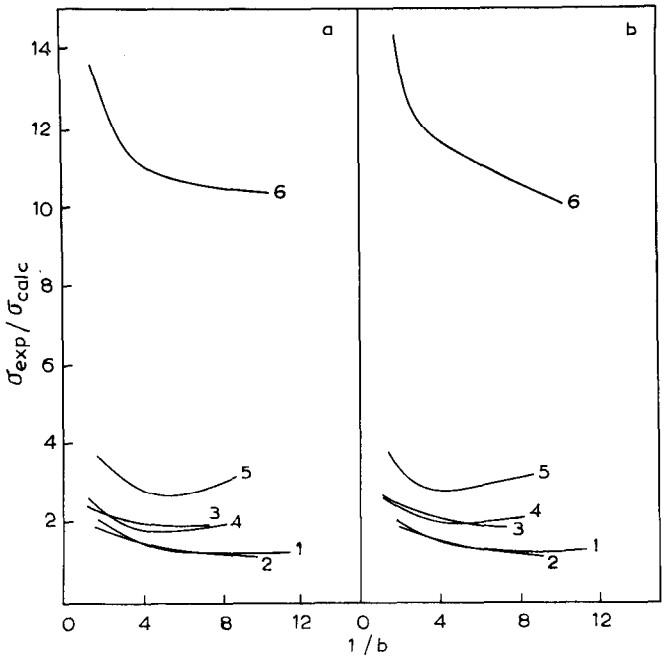

Fig. 8. Plot as in Fig. 2. Details and conditions equal to Fig. 2, with the same assumption as in Fig. 7 (N = 10 000 theoretical plates).

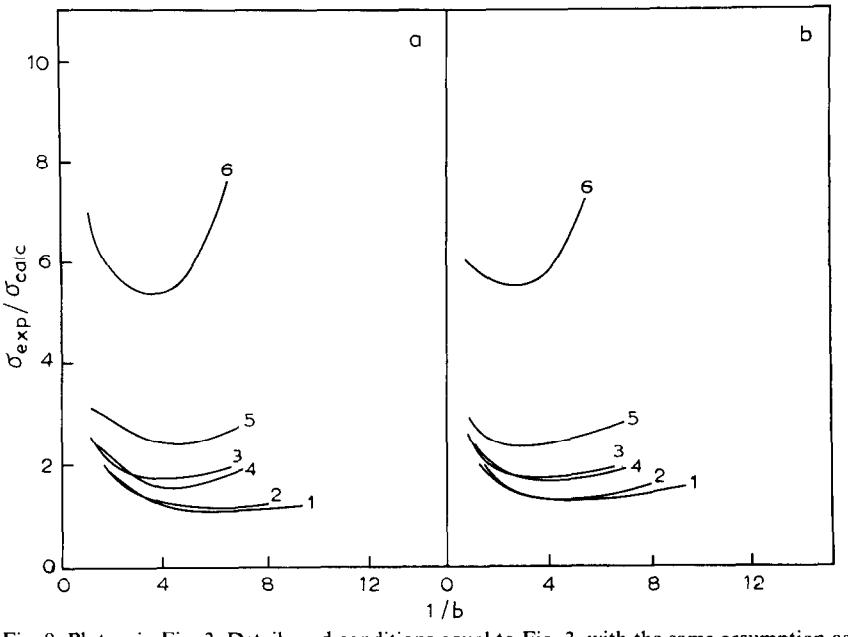

Fig. 9. Plot as in Fig. 3. Details and conditions equal to Fig. 3, with the same assumption as in Fig. 7 (N = 10 000 theoretical plates).

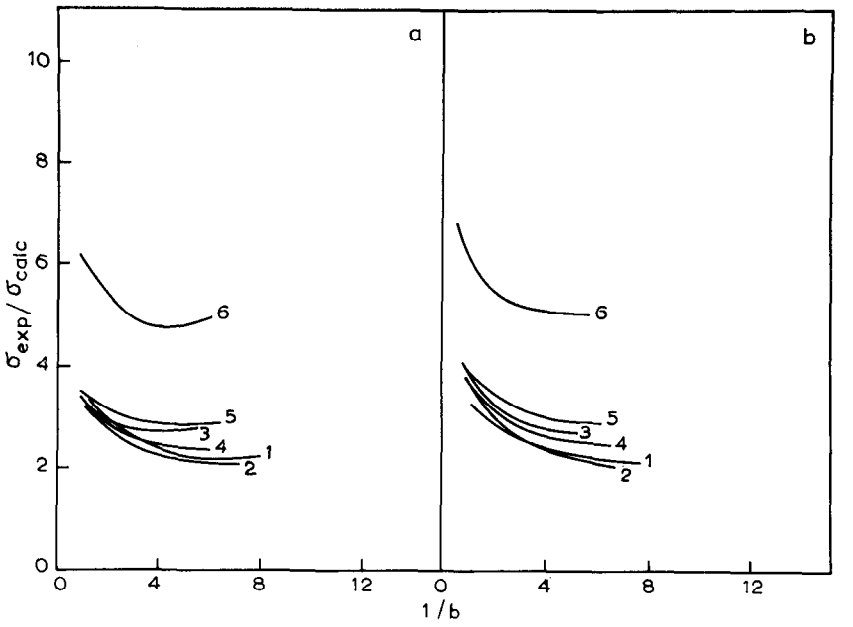

Fig. 10. Plot as in Fig. 4. Details and conditions equal to Fig. 4, with the same assumption as in Fig. 7 (N = 10 000 theoretical plates).

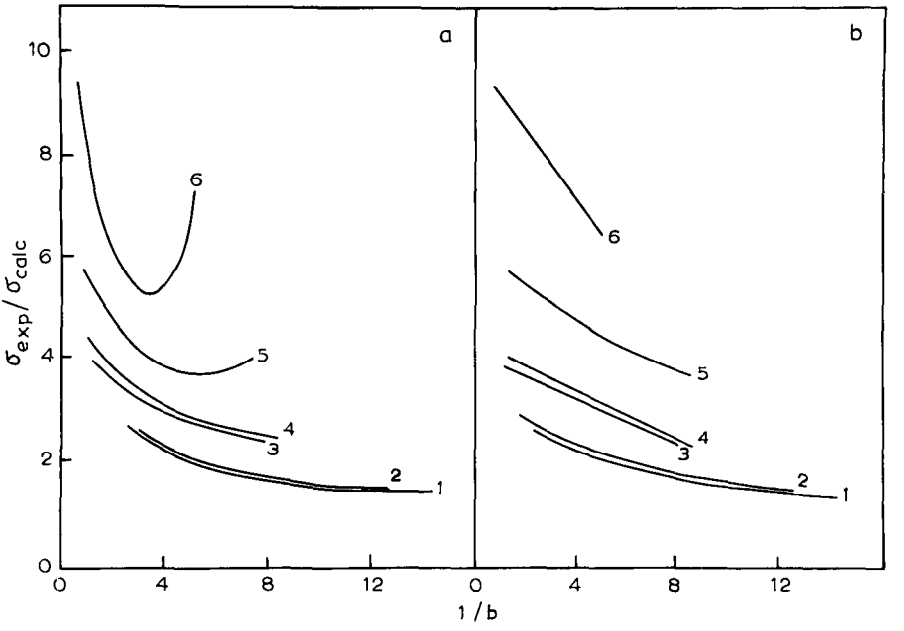

Fig. 11. Plot as in Fig. 5. Details and conditions equal to Fig. 5, with the same assumption as in Fig. 7 (N = 10 000 theoretical plates).

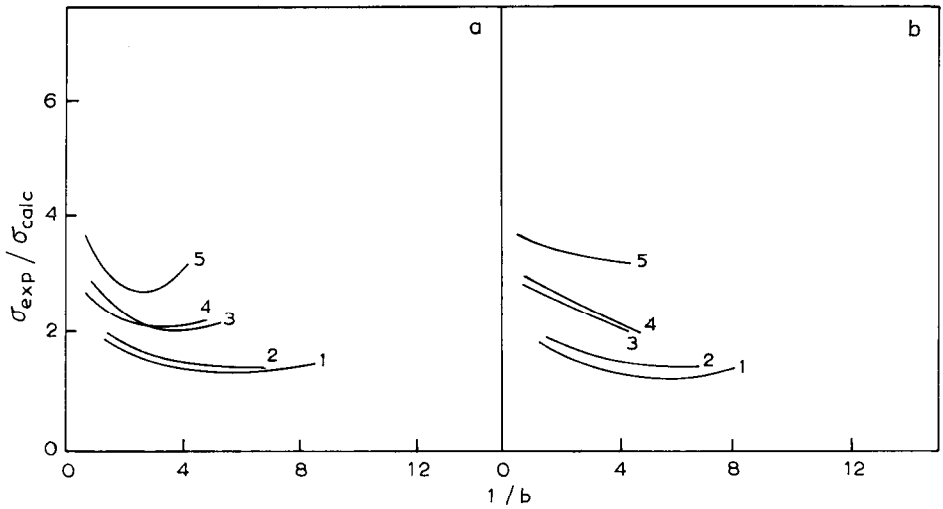

Fig. 12. Plot as in Fig. 6. Details and conditions equal to Fig. 6, with the same assumption as in Fig. 7 (N = 10 000 theoretical plates).

experimental variables. Major decreases in the value of N for a particular polypeptide would be expected from eqn. 29 when significant increases in the value of C occur in response to a change in an elution condition. For example, our previous studies[9] on phenylalanine oligomers and small proteins, separated on n-alkylsilicas, have shown similar pronounced dependencies of N on analysis time, the value of N rapidly decreasing (and hence h rapidly increasing) as k' was increased over a relatively small range, *i.e.* $\Delta k' \leqslant 0.5$.

The data in Figs. 1–6 permit several further comparisons to be made with regard to the effect of pore diameter and column configuration. According to eqn. 31, at a defined $\bar{k}$ value, *i.e.* for a specified b value, and fixed t_G, F, d_p, and $\Delta\varphi$ values, $\sigma_{v,calc}$ will decrease as the input S value of a particular polypeptide increases. As a consequence, the value of $\sigma_{v,exp}/\sigma_{v,calc}$ is expected to increase according to the relative S values of a peptide series when the value of $(C/D_m)^{0.5}$ remains constant over the operational range of b values. Since calculations of $\sigma_{v,calc}$ according to eqn. 30 or 31 take into account the effect on σ_v of the different elution times for the various solutes (through the $\bar{k}$ term) and the effects of the B and C coefficients (through the restricted and surface diffusion terms), solutes with smaller molecular topographies and S values under different gradient and column conditions should exhibit very similar and even superimposible plots of $\sigma_{v,exp}/\sigma_{v,calc}$ *versus* $1/b$.

In previous studies[9] we have shown that the S value of a polypeptide, separated on different porous n-alkylsilicas, remains essentially constant, provided that the ligand densities of the n-alkyl chains are similar. As can be seen from Table I, the derived S values for the β-endorphin polypeptides follow a similar pattern with this selection of stationary phases. Although the anticipated effect of the S value on the $\sigma_{v,exp}/\sigma_{v,calc}$ value is to some extent followed, it is evident from Figs. 1–6 that divergences in the expected order occur. For example, the data for peptides 1 and 5 show that their relative bandwidths change significantly, despite their similarity in sequence

and molecular weight. If all peptides could be represented by a single class of similarly shaped solutes, then the polypeptides listed in Table I could effectively be considered as three sets according to their molecular weights, *i.e.* peptides 1 and 2 as one set, peptides 3–5 as a second set, and peptide 6 as representative of a third set.

Clearly, the experimental data cannot be readily accommodated in terms of the effect of molecular weight *per se* on the solute diffusion coefficient. What then is the origin of the observed bandwidth differences between these sets of peptides with the various stationary phases of different pore diameter but similar *n*-alkyl chain ligand densities? Because of their sequence characteristics, the participation of additional coulombic or silanophilic effects can be largely discounted for peptides 1 and 2, or 3 and 4. In fact, as is evident from Figs. 1–6, the bandwidths of peptides 3 and 4 are very similar for all the stationary phases, except possibly the 30-nm pore diameter packing, where divergences at very small values of b are observed. As a consequence, it can be concluded that peptides 3 and 4 exhibit very similar, if not identical, conformation under all the chromatographic conditions examined.

Are the bandwidth differences between the peptide sets due to limited solubility? This possibility was also discounted early in this investigation from data on solubility measurements. Two candidate possibilities are currently favoured. The first possibility assumes that significant secondary structure changes occur at the intraparticulate boundary *vis-à-vis* sphere–cyclinder shape interconversions at the pore chamber exits. The second possibility assumes that these secondary structural effects are mediated, either exclusively or in synergy, at the stationary phase surface. Since the horizon of the stationary phase surface will be quite limited in terms of molecular distances, due to undulating fine-structure micropores, microchasms, etc., the manner in which a solute undergoing re-orientation at the surface can probe these stationary phase pore contours will be highly selective. In this context, the contrast between the Novapak C_{18} packing and the other octadecylsilica stationary phases is noteworthy. Also of interest are the different dependencies of the bandwidths for the studied polypeptides on the gradient steepness parameter when the results of the stainless-steel and radial-compression columns, packed with Novapak C_{18}, are compared. Essentially shallow dependencies of $\sigma_{v,exp}/\sigma_{v,calc}$ on $1/b$ were found for Novapak C_{18} in standard analytic stainless-steel columns, and much steeper dependencies when the same stationary phase was packed into radial-compression columns. Even when allowance is made for differences in reduced velocities between the two columns, the magnitude of the $\sigma_{v,exp}/\sigma_{v,calc}$ *versus* $1/b$ differences cannot be readily accommodated in terms of conventional kinetic theory of bandbroadening, unless the influence of relative residence times and dwell effects are also taken into account.

It can be concluded from the above results that, although current theory may allow chromatographic retention parameters, such as t_g, $\bar{k}$, S, etc., to be predicted with reasonable correlation with the experimental data, a similar situation with regard to the prediction of bandwidth data for solutes undergoing slow secondary equilibria is not yet at hand. This conclusion is further reinforced by examination of the plots of peak capacity (as calculated from eqns. 2 and 37) as a function of $\bar{k}^{0.25}/C^{0.5}$.

Comparison of observed and predicted peak capacities as a function of experimental variables

Eqn. 35 predicts a linear dependence of PC on $\bar{k}^{0.25}/C^{0.5}$. For a particular column and specified values of F and $\Delta\varphi$, the magnitude of PC at a defined value of $\bar{k}^{0.25}/C^{0.5}$ should also be proportional to the S value. Hence, linear plots of $(PC)_{calc}$ *versus* $\bar{k}^{0.25}/C^{0.5}$ are expected when experimentally derived values of $\bar{k}$, S, C, t_o, d_p, F, and $\Delta\varphi$ and D_m values, calculated according to eqns. 24–27 are used. When the bandwidth behaviour of polypeptides is in accord with the simple kinetic model inherent to eqn. 36, linear plots of $(PC)_{exp}$, derived from eqn. 2, *versus* $\bar{k}^{0.25}/C^{0.5}$ should also be expected. Figs. 13–18 show the plots of $(PC)_{calc}$ *versus* $\bar{k}^{0.25}/C^{0.5}$ and $(PC)_{exp}$ *versus* $\bar{k}^{0.25}/C^{0.5}$. Firstly, it is evident from Figs. 13a–18a that, with values of $\bar{k}$, C, and S, derived from experiments in which t_G = 20, 30, 40, 60 and 120 min at F = 1 ml/min, essentially linear plots of $(PC)_{calc}$ *versus* $\bar{k}^{0.25}/C^{0.5}$ are obtained. Secondly, the relative order of these plots is determined with some stationary phase systems but not all by the magnitude of the S parameter, *i.e.* as the magnitude of the experimen-

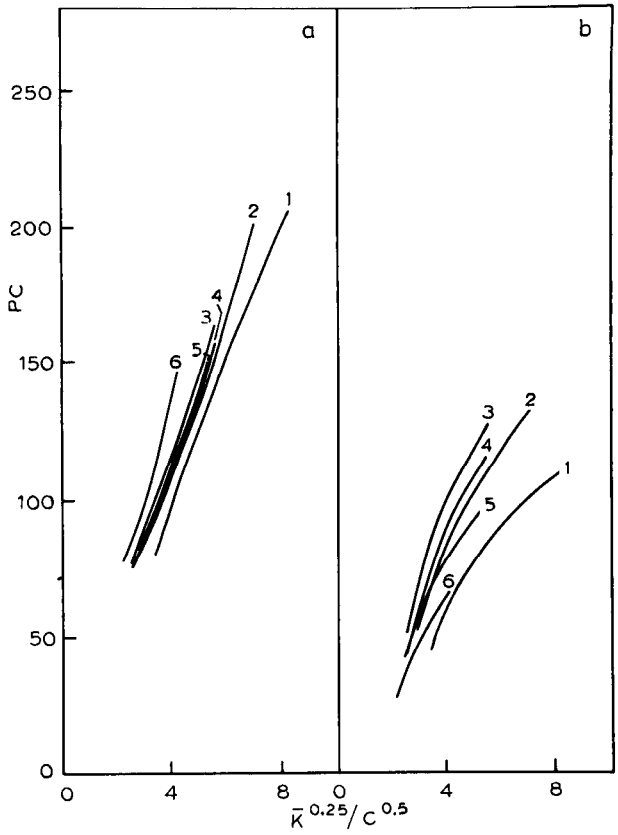

Fig. 13. Plots of peak capacity versus $\bar{k}^{0.25}/C^{0.5}$ for the human β-endorphin-related polypeptides 1–6. Conditions equal to Fig. 1. The peak capacity was calculated from eqn. 35 (panel a) or eqn. 2 (panel b). The plot was determined as curves of best fit with the ±10% standard deviation of all data points. The $\bar{k}$ and C values were computed by iterative non-linear least-squares averaging procedures and evaluated from eqns. 10 and 20.

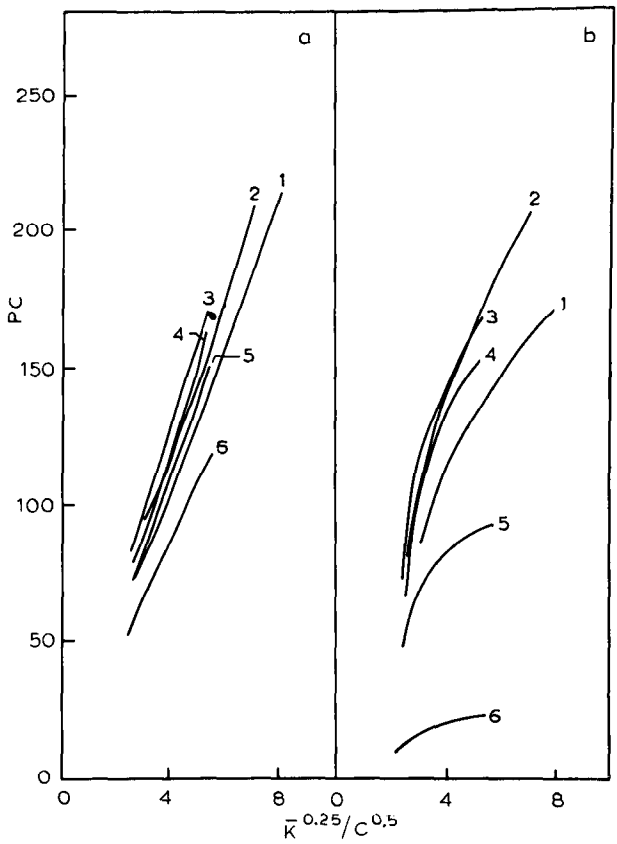

Fig. 14. Plot as in Fig. 13. Conditions equal to Fig. 2. Details as in Fig. 13.

tally determined value of the S parameter increases, the magnitude of $(PC)_{calc}$ at a particular value of $\bar{k}^{0.25}/C^{0.5}$ increases in accord with eqn. 35. As a consequence, improved resolution should be achieved with elution systems which generate large S values for different solutes, provided σ_v approaches its theoretical minimum and the $\Delta\varphi$ range can be easily defined. Thirdly, when solutes exhibit changes in bandspacing or selectivity reversals under different gradient conditions, as revealed in the log $\bar{k}$ *versus* $\bar{\varphi}$ plots[24], corresponding intercepts are found in the $(PC)_{calc}$ *versus* $\bar{k}^{0.25}/C^{0.5}$ plots. The slight curvature seen in these $(PC)_{calc}$ plots with certain $\bar{k}$ or C values presumably reflects the divergence from linearity of the dependence of log $\bar{k}$ on $\bar{\varphi}$ with the concomitant overestimation of the value of the S parameter at specific values of $\bar{k}$. For a defined value of $\bar{k}^{0.25}/C^{0.5}$, the corresponding value of $(PC)_{calc}$ can thus be considered to be the theoretical maximum PC value for that solute when eluted under a controlled set of chromatographic conditions.

Comparison of these data for the predicted behaviour of polypeptide band-broadening in reversed-phase systems with the data embodied in the plots of $(PC)_{exp}$ *versus* $\bar{k}^{0.25}/C^{0.5}$ (Figs. 13b–18b) is, consequently, most illuminating. As can be seen from the various figures, in all cases $(PC)_{exp}$ is smaller than $(PC)_{calc}$ over the same

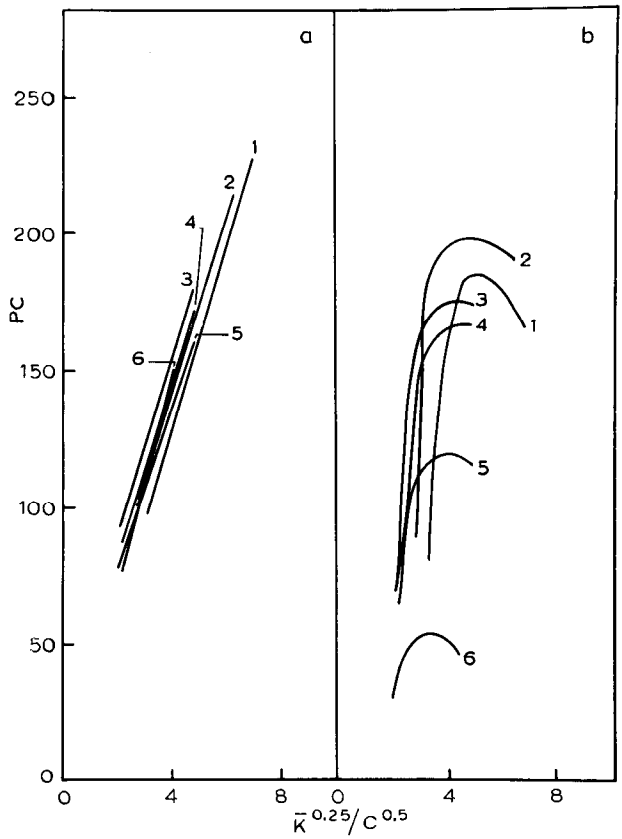

Fig. 15. Plot as in Fig. 13. Conditions equal to Fig. 3. Details as in Fig. 13.

range of values of $\bar{k}^{0.25}/C^{0.5}$. For the small peptides, the value of $(PC)_{calc}/(PC)_{exp}$ was *ca.* 1.20 ± 0.2 at a value of $\bar{k}^{0.25}/C^{0.5}$ of 4 for the different columns examined. However, for the larger polypeptides, this ratio increased significantly up to *ca.* 3.0 ± 0.5. The values of $(PC)_{exp}$ for the different peptides tend to decrease as the molecular complexity of the solute increases, although —even with a limited selection of polypeptide analogues as studied here— exceptions are evident, *e.g.* compare peptide 1 with peptide 2, or peptide 5 with peptide 6.

The influence of pore diameter and possibly also ligand density on peak capacity is also evident in these comparisons. Thus, with the four 6-μm octadecylsilica stationary phases of different porosities (7.3, 10, 13 and 30 nm) packed into stainless-steel columns of identical dimensions, $(PC)_{exp}$ for the smaller peptides appeared to improve with the stationary phases up to a mean pore diameter of 13 nm, whilst with the larger peptides, *i.e.* β-endorphin (6), $(PC)_{exp}$ was largest with the 30-nm pore-diameter octadecylsilica material. As expected on the basis of the differences in linear elution velocity, column dimensions, $\bar{k}$ and S, the $(PC)_{calc}$ values for the different polypeptides separated on the 4-μm Novapak octadecylsilica, packed into radial-compression modules, were larger than the values of $(PC)_{calc}$ for the corresponding stainless-steel column system. When F = 1.0 ml/min was used with both Novapak

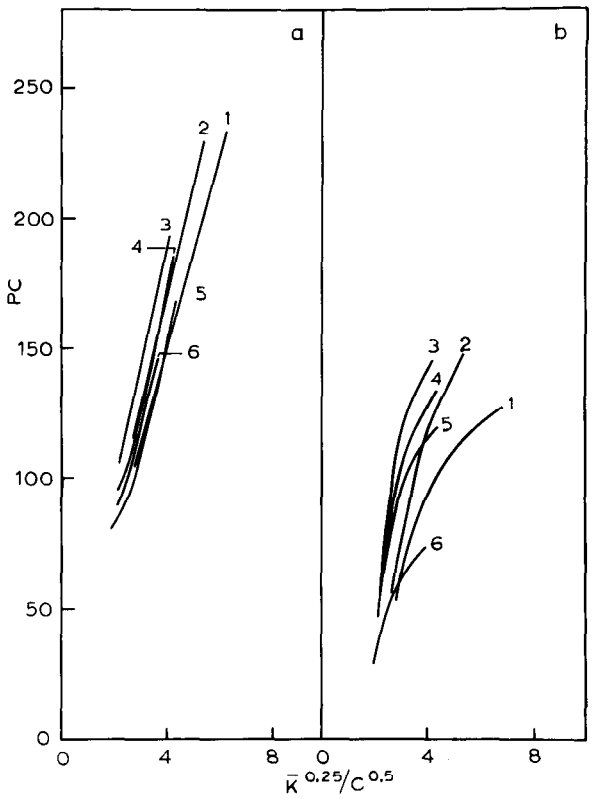

Fig. 16. Plot as in Fig. 13. Conditions equal to Fig. 4. Details as in Fig. 13.

columns, it was surprising [in view of the relationship between υ, L and V_m (eqn. 16)] to observe that the $(PC)_{exp}$ values for this group of polypeptides, separated on the stainless-steel column, were larger than those obtained for the radial-compression module, even after normalisation for column volume differences. Previously, we and others have shown[13,29] that, as the relative linear-flow velocity is decreased in reversed-phase isocratic and gradient-elution separations of polypeptides and proteins, the bandwidths, peak shape, and solute recovery do not necessarily improve, as may intuitively be expected. Low flow-rates can lead to significant protein loss on the column in reversed-phase chromatography. Similar results have recently been documented[38] for ion-exchange HPLC of proteins.

It can thus be concluded that the observed bandwidth behaviour of the small peptides 1 (MW 573), and 2 (MW 761) over a wide range of gradient conditions approaches the bandwidth behaviour predicted from well-established theory of zone dispersion in chromatographic systems. The question that then arises is why the larger polypeptides diverge so significantly. Is it due to the 0.1% trifluoroacetic acid in the eluent, the unique participation of silanophilic interactions between basic groups at *endo*-positions in the polypeptide and polar binding sites on the stationary phase surface, solute-dependent solvation equilibria that result in different but static geometric shapes for the various interacting polypeptides, or are there dynamic con-

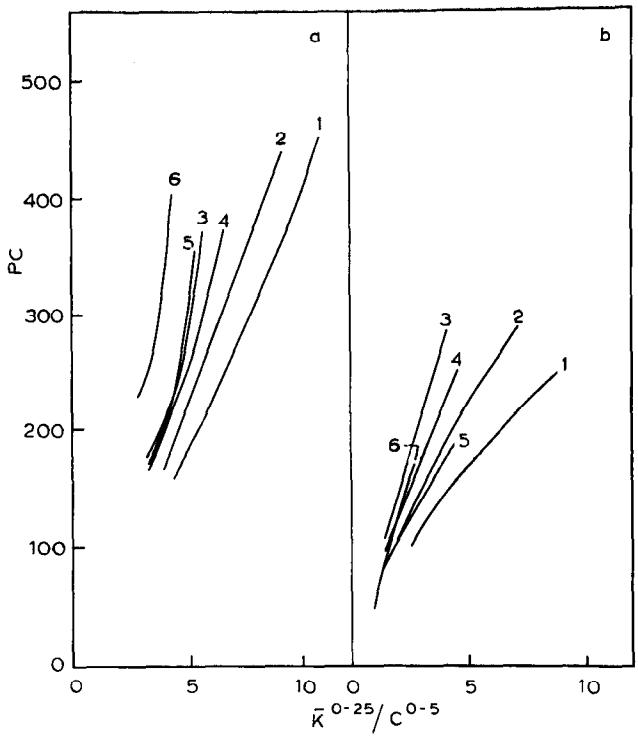

Fig. 17. Plot as in Fig. 13. Conditions equal to Fig. 5. Details as in Fig. 13.

formational processes occurring, even with these relatively small polypeptides? In this study, recoveries were uniformly high and there was no evidence to suggest that silanophilic effects were selectively occurring with only the large polypeptides. Solute solubility and relative differences in solute polarity do not appear to be an issue. In order to quantify the importance of the other two possibilities involving secondary structural changes, other analytical methods are required. To a very large extent, solute solvation, *i.e.* the nature of the water structure surrounding the solute, and solute conformation in the intraparticulate spaces and at the stationary phase surface, are intimately associated. It can be argued that the process of polypeptide binding to a hydrophobic surface, such as a porous *n*-alkylsilica reversed-phase material must involve displacement of previously bound solvent molecules from the stationary phase surface and from the solvated polypeptide itself. The energy required for this interaction may well come from unfolding/refolding processes and associated changes in the solute structure. These processes are time-dependent and may involve more than one discrete stage of solute re-orientation at the stationary phase surface. As a consequence, the solute will search out the minimum energy requirements for the particular environment in which it finds itself and, in so doing, must explore a variety of conformational options. If the relaxation times for these conformational changes are similar to the time of analysis, peak broadening will occur. A growing body of evidence is becoming available on the importance of such phenomena for polypeptides separated on *n*-alkylsilicas, including studies on *cis/trans* rearrangement for

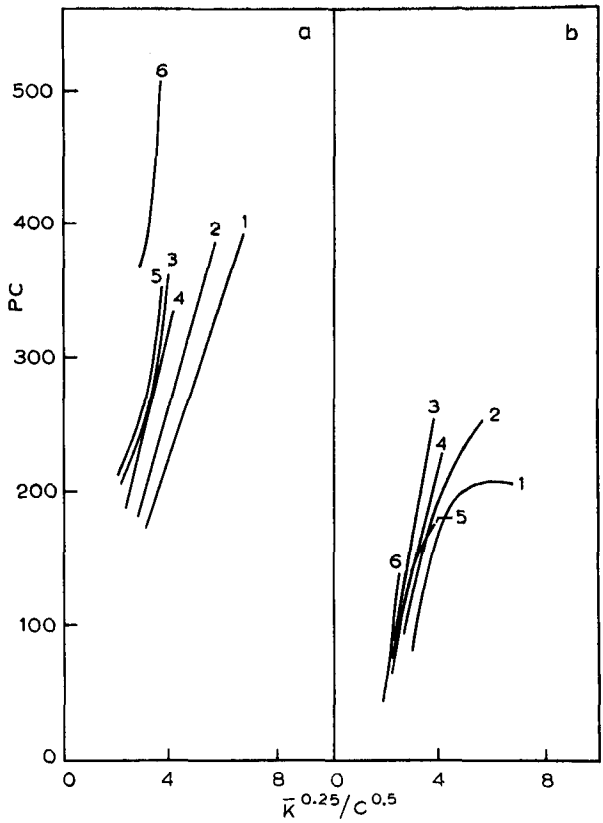

Fig. 18. Plot as in Fig. 13. Conditions equal to Fig. 6. Details as in Fig. 13.

prolinyl peptides[43], as well as unfolding/denaturation of a number of proteins, including soyabean trypsin inhibitor, trypsin, and ribonuclease[29,44]. In the case of β-endorphin-related peptides, subsequent studies in this laboratory have all been in accord with the conclusion that a stabilized C-terminal amphiphilic α-helix is generated with peptide 6, but not with peptides 1–4 under interactive hydrophobic conditions. Other investigations to be reported subsequently[45] with luteinising hormone releasing factor and growth hormone releasing factor indicate that β-bends can similarly be stabilised at the hydrophobic *n*-alkylsilica surface. As a consequence, such kinetic behaviour must be considered to be a general phenomenon for all peptides that have the ability to generate secondary or higher structures with relatively large half lives, *i.e.* $t_{0.5} \gg 1$ s, in solution or at a liquid–solid interface. Elution conditions can certainly be chosen to minimise these competing effects (*e.g.*, refs. 7, 8 and 38) at the expense of biological recovery, but in view of the time-dependent nature of these phenomena, it is likely that in complex polypeptide mixtures some components may still show so-called "anomalous" behaviour. In fact, the observed bandbroadening behaviour in these cases is entirely consistent with the secondary and tertiary structures of the solutes. As a consequence, analysis of the dependence of these kinetic processes on experimental variables should prove a very fruitful area of investigation

on the dynamic properties of polypeptides at non-polar surfaces, from the chromatographic as well as the structure–function point of view.

ACKNOWLEDGEMENTS

This investigation was supported by the National Health and Medical Research Council of Australia under grants to M.T.W.H.

The generous assistance of Dr. J. van Nispen in providing the human β-endorphin analogues used in this study is also gratefully acknowledged. These investigations were initiated during the tenure of a grant made to M.T.W.H. by the Department of Science and the National Science Foundation under the Australia–United States Co-operative Science Programme.

LIST OF SYMBOLS

A	Knox equation constant due to packing irregularities in the column bed
a	Intercept of the B *versus* $\bar{k}$ plot, taken to be equal to 1.1
B	Knox equation constant, which arises from zone dispersion due to longitudinal diffusion
b	Gradient steepness parameter, as defined by eqn. 5
b'	Surface diffusion parameter, evaluated from the slope of the B *versus* $\bar{k}$ plot and related to D_s/D_m
C	Knox equation constant, which accounts for mass transfer contributions
D_m	Diffusion coefficient (cm^2/s) of the solute in the mobile phase
D_p	Effective intraparticulate diffusion coefficient (cm^2/s) within the pores of the packing material
D_s	Diffusion coefficient (cm^2/s) of the solute at the stationary-phase surface
d_p	Mean particle diameter (cm)
d_q	Mean pore diameter (cm)
d_s	Stokes diameter (cm) of the solute, equivalent to *ca.* 110% of the molecular diameter
F	Flow-rate of the mobile phase (ml/s)
G	Band compression factor, as defined by eqn. 4
h	Reduced plate height equal to L/Nd_p
$\bar{k}$	Instantaneous capacity factor of the solute as it traverses the midpoint of the column
k_c	Boltzmann constant (J/K)
k_0	Capacity factor determined or extrapolated at $\varphi = 0$
L	Column length (cm)
MW	Molecular weight (g) of the solute
N	Column plate number
PC_{exp}	Peak capacity, as defined by eqn. 2, from experimental values of t_G and $\sigma_{v,exp}$
PC_{calc}	Peak capacity, as defined by eqn. 35
R_s	Average resolution for gradient separation
S	Slope of the plot of log k' *versus* φ
T	Absolute temperature (K)

t_e	Gradient elapse time (s)
t_G	Gradient time (s)
t_g	Gradient elution time (s) of the solute
t_o	Column dead time (s)
t_s	Retention time (s) for the solute, eluted solely under size-exclusion conditions
V_m	Column void volume (ml)
V_{mv}	Molecular volume of the solute
x	Fraction of the column void volume in the interstitial spaces of the column bed
$\bar{\alpha}$	Gradient separation factor, as defined by the ratio of $\bar{k}$ values for two adjacent solute zones
β	Ratio of gradient times, as defined by $\beta = t_{G2}/t_{G1}$
γ	Packing obstruction factor
$\Delta\varphi$	Change in organic solvent modifier mole fraction
$\Delta \log \bar{k}$	Difference in logarithmic median capacity factor for a specified $\Delta\varphi$ change
η	Mobile phase viscosity at a defined temperature (poise)
Θ'	Rate of change of organic solvent modifier with time ($\Theta' = \Delta\varphi/t_G$)
υ	Reduced velocity of the mobile phase, given by LFd_p/V_mD_m
ρ	Ratio of the Stokes diameter of the solute to pore diameter of the particle
ρ^*	Restricted diffusion parameter
σ_t	Peak bandwidth in time units (s)
σ_t^2	Peak variance in time units
$\sigma_{v,exp}$	Peak bandwidth in volume units (ml), determined experimentally
$\sigma_{v,calc1}$	Peak bandwidth in volume units (ml), calculated according to eqn. 30
$\sigma_{v,calc2}$	Peak bandwidth in volume units, calculated according to eqn. 31
φ	Mole fraction of organic solvent modifier
τ_i	Average relaxation time for the interconversion of conformational species

REFERENCES

1 A. Henschen, H. P. Huppe, F. Lottspeich and W. Voelter, *High Performance Liquid Chromatography of Proteins and Peptides*, Springer Verlag, Berlin, 1984.
2 *J. Chromatogr.*, 266 (1983) entire volume.
3 *J. Chromatogr.*, 296 and 297 (1984) entire volumes.
4 *J. Chromatogr.*, 316 and 317 (1985) entire volumes.
5 M. T. W. Hearn, *Adv. Chromatogr.*, 20 (1982) 1.
6 M. T. W. Hearn, *Methods Enzymol.*, 104 (1984) 190.
7 M. T. W. Hearn, *Ion Pair Chromatography*, Marcel Dekker, New York, 1985, p. 207.
8 M. T. W. Hearn, in Cs. Horváth (Editor), *HPLC—Advances and Perspectives*, Vol. 3, Academic Press, New York, 1983, pp. 87–155.
9 M. T. W. Hearn and B. Grego, *J. Chromatogr.*, 296 (1984) 61.
10 J. D. Pearson and F. E. Regnier, *J. Liq. Chromatogr.*, 6 (1983) 497.
11 J. D. Pearson, N. T. Lin and F. E. Regnier, *Anal. Biochem.*, 124 (1982) 217.
12 M. J. O'Hare, M. W. Capp, E. C. Nice, N. H. C. Cooke and B. G. Archer, *Anal. Biochem.*, 126 (1982) 17.
13 E. C. Nice, M. W. Capp, N. H. C. Cooke and M. J. O'Hare, *J. Chromatogr.*, 218 (1981) 569.
14 N. H. C. Cooke, B. G. Archer, M. J. O'Hare, E. C. Nice and M. W. Capp, *J. Chromatogr.*, 255 (1983) 115.

15 M. T. W. Hearn and B. Grego, *J. Chromatogr.*, 282 (1983) 541.
16 M. T. W. Hearn and B. Grego, *J. Chromatogr.*, 255 (1983) 125.
17 L. A. Witting, D. J. Gisch, R. Ludwig and R. Eksteen, *J. Chromatogr.*, 296 (1984) 97.
18 K. A. Cohen, J. Chazaud and G. Calley, *J. Chromatogr.*, 282 (1983) 423.
19 J. A. Smith and M. J. O'Hare, *J. Chromatogr.*, 299 (1984) 13.
20 G. Lindgren, B. Lundström, I. Källman and K.-A. Hansson, *J. Chromatogr.*, 296 (1984) 83.
21 H. Englehardt, personal communication.
22 R. V. Lewis and D. DeWald, *J. Liq. Chromatogr.*, 5 (1982) 1367.
23 M.-I. Aguilar, A. N. Hodder and M. T. W. Hearn, *J. Chromatogr.*, 327 (1985) 115.
24 M. A. Stadalius, H. S. Gold and L. R. Snyder, *J. Chromatogr.*, 296 (1984) 31.
25 H. Colin, J. C. Diez-Masa, G. Guiochon, T. Czajkoska and I. Miedziak, *J. Chromatogr.*, 167 (1978) 41.
26 M. T. W. Hearn, unpublished results.
27 N. T. Miller and B. L. Karger, *J. Chromatogr.*, 326 (1985) 45.
28 L. R. Snyder, in Cs. Horváth (Editor), *HPLC —Advances and Perspectives*, Vol. 1, Academic Press, New York, 1980, pp. 208–316.
29 M. T. W. Hearn, M. I. Aguilar and A. N. Hodder, *J. Chromatogr.*, 327 (1985) 47.
30 M. J. O'Hare and E. C. Nice, *J. Chromatogr.*, 171 (1979) 209.
31 E. M. Renkin, *J. Gen. Physiol.*, 38 (1954) 225.
32 J. C. Giddings, *Dynamics of Chromatography*, Marcel Dekker, New York, 1965, p. 12.
33 J. C. Giddings, *Adv. Chromatogr.*, 20 (1982) 217.
34 C. R. Wilke and P. Chang, *AIChEJ*, 1 (1955) 264.
35 M. E. Young, P. A. Carroad and R. L. Bell, *Biotechnol. Bioeng.*, 22 (1980) 947.
36 M. T. W. Hearn, in preparation.
37 J. E. Bolton, J. H. Livesey and M. T. W. Hearn, *J. Liq. Chromatogr.*, 7 (1984) 1089.
38 M. T. W. Hearn and A. N. Hodder, submitted for publication.
39 M. A. Stadalius, H. S. Gold and L. R. Snyder, *J. Chromatogr.*, 327 (1985) 27.
40 M. A. Phelan and K. A. Cohen, *J. Chromatogr.*, 266 (1983) 55.
41 J.L. Meek and Z. L. Rossetti, *J. Chromatogr.*, 211 (1981) 15.
42 M. T. W. Hearn, P. G. Stanton and J. D. Davies, submitted for publication.
43 J. Jacobsen, W. Melander, G. Vaisnys and G. Horvath, *J. Phys. Chem.*, 88 (1984) 4536.
44 S. A. Cohen, Y. Tapuhi, J. C. Ford and B. L. Karger, *Anal. Chem.*, 56 (1984) 217.
45 M. T. W. Hearn and M. I. Aguilar, *J. Chromatogr.*, submitted for publication.